Biochemical characterization and mutational analysis of a novel flap endonuclease 1 from Thermococcus barophilus Ch5

Tan Lin, Likui Zhang, Donghao Jiang, Leilei Wu, Kaige Chen, Li Li, Cuili Jin, Zheng Li, Phil M. Oger

Biochemical characterization and mutational analysis of a novel flap endonuclease 1 from Thermococcus barophilus Ch5

Tan Lin, Likui Zhang, Donghao Jiang, Leilei Wu, Kaige Chen, Li Li, Cuili Jin, Zheng Li, Philippe Oger

Biochemical characterization and mutational analysis of a novel flap endonuclease 1 from *Thermococcus barophilus* Ch5

Tan Lin[1], Likui Zhang[1#], Donghao Jiang[1], Leilei Wu[1], Kaige Chen[1], Li Li[1], Cuili Jin[1,2], Zheng Li[3], and Philippe Oger[4#]

[1]College of Environmental Science and Engineering, Marine Science & Technology Institute, Yangzhou University, China

[2]Jiangsu Key Laboratory of Marine Bioresources and Environments, Jiangsu Ocean University, China

[3]College of Plant Protection, Agricultural University of Hebei, Baoding, China

[4]Univ Lyon, INSA de Lyon, CNRS UMR 5240, Villeurbanne, France

[#]Corresponding author: Dr. Likui Zhang

E-mail address: lkzhang@yzu.edu.cn

[#]Corresponding author: Dr. Philippe Oger

E-mail address: philippe.oger@insa-lyon.fr

ABSTRACT

Flap endonuclease 1 (FEN1) plays important roles in DNA replication, repair, and recombination. Herein, we report the biochemical characteristics and catalytic mechanism of a novel FEN1 from the hyperthermophilic euryarchaeon *Thermococcus barophilus* Ch5 (Tb-FEN1). As expected, the recombinant Tb-FEN1 can cleave 5′-flap DNA. However, the enzyme has no activity on cleaving pseudo Y DNA, which sharply contrasts with other archaeal and eukaryotic FEN1 homologs. Tb-FEN1 retains 24% relative activity after heating at 100°C for 20 min, demonstrating that it is the most thermostable among all reported FEN1 proteins. The enzyme displays maximal activity in a wide range of pH from 7.0 to 9.5. The Tb-FEN1 activity is dependent on a divalent metal ion, among which Mg^{2+} and Mn^{2+} are optimal. Enzyme activity is inhibited by NaCl. Kinetic analyses estimated that the activation energy for the removal of 5′-flap from DNA by Tb-FEN1 was 35.7 ± 4.3 kcal/mol, which is the first report on the energy barrier for excising 5′-flap from DNA by a FEN1 enzyme. Mutational studies demonstrate that the K87A, R94A and E154A amino-acid substitutions abolish cleavage activity and reduce 5′-flap DNA binding efficiencies, suggesting that residues K87, R94, and E154 in Tb-FEN1 are essential for catalysis and DNA binding as well. Overall, Tb-FEN1 is an extremely thermostable endonuclease with unusual features.

Keywords: Hyperthermophilic Archaea; Flap endonuclease 1; DNA replication and repair; Biochemical characteristics; Mutational studies

1. Introduction

Flap endonuclease 1 (FEN1), a structure specific nuclease, catalyzes the removal of 5′-flap from 5′-bifurcated DNA structures during DNA replication, repair, and recombination (Balakrishnan and Bambara, 2013), making this endonuclease fundamental in several essential biological processes. Indeed, FEN1 has been shown to excise RNA primers to process the Okazaki fragments during DNA replication (Bambara et al, 1997). In the long-patch base excision repair, FEN1 plays a role in removing damaged nucleotides (Klungland and Lindahl, 1997). Furthermore, FEN1 can facilitate homologous recombination by removing divergent sequences at DNA break ends (Kikuchi et al., 2005). In addition, FEN1 has also been implicated in other pathways such as non-homologous end joining, stalled replication fork rescue, apoptotic DNA fragmentation, and α-segment error editing (Wu et al., 1999; Zheng et al., 2011; Liu et al., 2015). Besides, FEN1 is also crucial for genomic stability in eukaryotes (Dehé and Gaillard, 2017; Tsutakawa et al., 2017). Thus, FEN1 is a central component of DNA metabolism since it can be involved in various DNA metabolic pathways (Liu et al., 2004). Additionally, FEN1 can be used as a novel diagnostic, prognostic biomarker and therapeutic target for cancer and gene editing (Varshney and Burgess, 2016; Xu et al., 2016; Guo et al., 2020; Zhao et al., 2020).

FEN1 is a member of the newly emerging family of structure-specific endonucleases that are evolutionarily ubiquitous in Archaea and Eukarya (Lieber, 1997; Shen et al., 1998). FEN1 possesses flap endonuclease activity as well as 5′→3′ exonuclease activity that allows it to remove RNA primers during lagging strand

synthesis in DNA replication and damaged DNA fragments in various DNA repair pathways. Structural and biochemical data have provided a wealth of information about structure-function relationship of FEN1 (Finger et al., 2012; Grasby et al., 2012). The crystal structures of FEN1 homologs demonstrate that a conserved helical arch harbors the active site (Ceska et al., 1996; Hosfield et al., 1998b; Hwang et al., 1998; Chapados et al., 2004). Besides, a flexible loop is essential for flap cleavage since the 5′-end of the DNA flap could thread through the hole of the loop tracking the length of the 5′-tail (Murante et al., 1995; Storici et al., 2002; Chapados et al., 2004; Shi et al., 2017).

As one of the ancestors of Eukarya, Archaea are an ideally simplified model for many aspects of DNA replication and repair in Eukarya. Since the first FEN1 from the hyperthermophilic euryarchaeon *Methanococcus jannaschii* was structurally characterized (Hosfield et al., 1998a; Hwang et al., 1998; Rao et al., 1998; Bae et al., 1999), several FEN1 homologs have been reported from other hyperthermophilic Archaea (HA), including *Archaeoglobus fulgidus* (Chapados et al., 2004; Hosfield et al., 1998a), *Pyrococcus horikoshii* (Matsui et al., 1999; Matsui et al., 2014; Matsui et al., 2002), *Pyrococcus furiosus* (Hosfield et al., 1998a; Hosfield et al., 1998b; Allawi et al., 2003), *Thermococcus kodakarensis* (Burkhart et al., 2017; Muzzamal et al., 2020), *Desulfurococcus amylolyticus* (Mase et al., 2011), *Aeropyrum pernix* (Collins et al., 2004), *Sulfolobus tokodaii* (Horie et al., 2007) or *Sulfolobus solfataricus* (Beattie and Bell, 2012). The FEN1 homologs from HA have two common characteristics: thermostability and thermophilicity, capable of cleaving DNA at high temperature. Like eukaryotic FEN1, the homologs from HA also utilize a two divalent metal ion

mechanism for catalysis. These two divalent metal ions are bound by highly conserved acidic amino acids at the bottom of a positively charged cleft to form a complex, among which one metal ion is presumably responsible for catalysis and the other for substrate binding (Shen et al., 1996). However, the FEN1 proteins from HA harbor characteristics distinct from the eukaryotic and other archaeal homologs, which comprise varied substrate specificity, tolerance to acidic pH and elevated temperatures, dependency to different metal ions and salt tolerance. For example, the *M. jannaschii* FEN1 functions effectively at high salt concentrations, which contrasts with the eukaryotic FEN1 (Horie et al., 2007). Although the overall structures of FEN1s from several HA are similar to those of eukaryotic FEN1 proteins (Matsui et al., 2002; Mase et al., 2011), they possess subtle conformational differences. For instance, the conformation of the putative substrate-binding pocket of the FEN1 from the hyperthermophilic archaeon *D. amylolyticus* is unique and created by a helical clamp and a flexible loop (Mase et al., 2011). The crystal structure of FEN1 from the hyperthermophilic archaeon *P. horikoshii* also demonstrates that its active cleft is formed by one large loop and four small loops (Matsui et al., 2002).

Relatively few FEN1 proteins from the hyperthermophilic genus *Thermococcus* have been investigated to date. Recent genetic studies have shown that the Δ*fen1 T. kodakarensis* mutant grows well, suggesting that FEN1 has no discernible effect on viability and growth of this archaeon (Burkhart et al., 2017). Further biochemical data demonstrate that the *T. kodakarensis* FEN1 displays maximal activity for excising 5′-flap from DNA at 80°C and at pH 7.5 (Muzzamal et al., 2020).

Thermococcus barophilus Ch5 is an anaerobic thermo-piezophilic archaeon, which was isolated from a deep-sea hydrothermal field of the Mid-Atlantic Ridge (Logachev field chimney, 3,020 m depth), growing optimally at 88°C under 40 MPa of hydrostatic pressure (Kim et al. Nature 2010). *T. barophilus* Ch5 possesses a putative FEN1 (Oger et al., 2016). In this work, we report the gene cloning, characterization, and mutational studies of a FEN1 from *T. barophilus* Ch5 (Tb-FEN1), showing that the enzyme is a quite thermostable endonuclease with unusual features. Importantly, we report for the first time the activation energy required for 5′-flap DNA removal by a FEN1 enzyme.

2. Materials and methods

2.1. Materials

Plasmid Extraction Kit, PCR Cycle Pure Kit, Gel Extraction Kit, and the competent *Escherichia coli* DMT cells were purchased from Transgene (Beijing, China); T4 DNA ligase, *Bam*HI, and *Xho*I were purchased from Thermo Scientific (Waltham, MA). High-fidelity PCR Mix was purchased from Vazyme (Nanjing, China). Chemicals were purchased from Amresco (WA, USA).

2.2. Cloning, expression, and purification of Tb-FEN1

The Tb-FEN1 gene (TBCH5v1_1306) was amplified from *T. barophilus* Ch5 genomic DNA with High-Fidelity PCR Mix with the specific primers containing *Bam*HI and *Xho*I restriction sites (Tb-FEN1 F and Tb-FEN1 R, Table 1). After DNA denaturation at 95°C for 3 min, the amplified PCR reaction was performed by following 34 cycles of 95°C for 30 s, 55°C for 30 s, and 72°C for 1 min, with a final extension

step at 72°C for 5 min. After digestion with *BamH*I and *Xho*I, the amplified DNA product was ligated into the pET-28at-plus vector digested with the same two enzymes to produce a recombinant Tb-FEN1 gene with a 6 x His-tag at the C-terminus. The construction was verified by sequencing and then transformed into the expression strain *E. coli* BL21 (DE3) RIL cells for protein expression.

The Tb-FEN1 gene was expressed in LB medium with 100 μg/mL kanamycin and 34 μg/mL chloramphenicol by the addition of isopropyl thiogalactoside (IPTG) at a final concentration of 0.1 mM when the OD_{600} of the expression strain *E. coli* reached 0.6 at 37°C. The culture was further incubated for about 10 hrs at room temperature under agitation.

The culture was harvested by centrifugation (6000×g for 15 min at 25°C) and the pellet was resuspended in Ni column buffer A (20 mM Tris-HCl pH 8.0, 1 mM dithiothreitol (DTT), 500 mM NaCl, 50 mM imidazole, and 10% glycerol). The cells were disrupted by sonication on ice and the supernatant was harvested into a 50 mL tube by centrifugation (16000×g for 30 min at 4°C). To remove non-thermostable *E. coli* nuclease activities, the supernatant was heated at 70°C for 20 min and then collected by centrifugation at 16000×g for 30 min at 4°C. The resulting supernatant was loaded into a HisTrap FF column (GE Healthcare, Uppsala, Sweden) using NCG™ Chromatography System (Bio-Rad, Hercules, CA, USA) and then the Tb-FEN1 protein was eluted in a linear gradient of 50–500 mM imidazole. The collected fractions harboring the Tb-FEN1 protein were verified by electrophoresis in a 12% SDS-PAGE. The purified Tb-FEN1 protein was dialyzed against a storage buffer (20 mM Tris-HCl

pH 8.0, 50 mM NaCl, 1 mM DTT, and 50% glycerol) and stored at -80°C. Based on the molar extinction coefficient of the Tb-FEN1 protein (43,890 M^{-1} cm^{-1}), the Tb-FEN1 protein concentration was determined by measuring the absorbance at 280 nm.

2.3. Construction, expression, and purification of the Tb-FEN1 mutants

The Tb-FEN1 N30M, K87A, R94A, E154A, Q172E, Y174M, R186A, N187H, L226F, D236A and N238C mutants were engineered using the plasmid harboring the wild-type Tb-FEN1 gene as template with a Site-directed Mutagenesis Kit according to the manufacturer's instructions. The sequences of the mutagenic primers are listed in Table 1. After verification of the contructs by sequencing, the Tb-FEN1 mutant proteins were overexpressed, purified, and quantified as described above for the wild-type protein.

2.4. DNA cleavage assays

The oligonucleotides were synthesized by Sangon Biotech Company, China. Oligonucleotide sequences are listed in Table S1. The Cy3-labeled oligonucleotide was annealed with the appropriate complementary oligonucleotides in buffer (20 mM Tris–Cl pH 8.0 and 100 mM NaCl) to prepare 5′-flap, pseudo Y DNA or dsDNA (Table S2). The annealing reactions were performed at 100ºC for 3 min, and cooled down slowly to room temperature at least 4 hrs.

The standard Tb-FEN1 DNA cleavage reactions were performed in reactions (10 μL) containing 20 mM Tris–HCl pH 8.0, 1 mM DTT, 8% glycerol, 100 nM Cy3-labeled 5′-flap DNA and 1000 nM Tb-FEN1 at 45°C for 30 min, unless stated otherwise. 10 μL of stop solution containing 98% formamide and 20 mM EDTA (Ethylene Diamine

Tetraacetic Acid) was added to stop the reactions. After denaturation at 95°C for 5 min and rapid cooling on ice for 5 min, the cleaved product was separated by electrophoresis in a denaturing 15% polyacrylamide gel containing 8 M urea in 0.5 × TBE (Tris-Borate-EDTA). Quantitative analysis was performed with the ImageQuant software after imaging the gels with a molecular image analyzer (PharosFx System, BioRad). All DNA cleavage assays were replicated three times.

2.5. Biochemical characterization assays

To investigate the biochemical characteristics of the 5′-flap DNA we used in this work, including its thermostability, optimal pH, divalent metal ion requirement and salt tolerance, we performed DNA cleavage reactions catalyzed with Tb-FEN1 in various conditions. To determine the thermostability of the enzyme, the Tb-FEN1 protein was heated at 85ºC, 90ºC, 95ºC and 100ºC for 20 min, respectively. After heating, the Tb-FEN1 protein was used to perform the DNA cleavage reactions under standard conditions.

The optimal pH-dependence of the Tb-FEN1 activity was examined by performing the DNA cleavage reactions at various pHs (6.5, 7.0, 7.5, 8, 8.5, 9, 9.5 and 10). The corresponding pHs were prepared using five different buffers (all at 20 mM concentrations) as follows: sodium phosphate-NaOH (pH 6.5, 7.0 and pH 7.5), Tris–HCl (pH 8.0 and 8.5), and Glycine -NaOH (pH 9.0, pH 9.5 and pH 10.0). The reaction products were treated as described above.

We investigated the effects of divalent metal ions on the Tb-FEN1 activity by performing the DNA cleavage reactions in presence of 5 mM of either Mg^{2+}, Mn^{2+},

Ca^{2+}, Zn^{2+}, Co^{2+}, Ni^{2+}, or Cu^{2+}. The reaction products were treated as described above.

We determined the effect of salinity on Tb-FEN1 activity by performing the DNA cleavage reactions at various NaCl concentrations ranging from 50 to 1000 mM. The reaction products were treated as described above.

2.6. DNA-binding assays

DNA-binding assays were performed by incubating the wild-type and mutant Tb-FEN1 with 100 nM 5′-flapped DNA in buffer (10 μL) containing 20 mM Tris-HCl pH 8.0, 1 mM DTT, and 8% glycerol at 25°C for 10 min. The free DNA substrate and bound DNA product with the wild-type and mutant Tb-FEN1 were separated by electrophoresis in a 4% native polyacrylamide gel in 0.1 × TBE buffer. Quantitative analysis was performed with the ImageQuant software after the gels were scanned with a molecular image analyzer (PharosFx System, BioRad). DNA binding assays were repeated three times.

2.7. Kinetic analysis

Under the single-turnover conditions where Tb-FEN1 (1000 nM) is 10-fold higher than 5′-flap DNA (100 nM), the DNA cleavage assays were performed at varied temperatures for various times. The calculated concentrations of the remaining substrate after DNA cleavage by Tb-FEN1 were fitted using KaleidaGraph (Synergy Software) by a single exponential decay equation:

$$[\text{Remaining substrate}] = A \exp(-k_{endo}t)$$

where A and k_{endo} are the reaction amplitude and the cleavage rate, respectively.

The measured k_{endo} values at varied temperatures were treated to be Ln k_{endo},

according to an Arrhenius Equation:

$$k_{endo} = A_r [\exp(-E_a/RT)]$$

where Ar, E_a, R, and T represent a proportionality constant, the activation energy, the universal gas constant, and reaction temperature in Kelvin, respectively. An activation energy was yielded by plotting the treated k_{endo} values (Ln k_{endo}) at varied temperatures with the treated reciprocal of reaction temperature (1000/K) by a linear regression.

3. Results

3.1. The genome of T. barophilus Ch5 encodes a putative FEN1

The genome of *T. barophilus* Ch5 encodes a putative flap endonuclease 1 (gene TBCH5v1_1306, accession number WP_056933915.1), belonging to the structure-specific nuclease superfamily. The sequence alignment of Tb-FEN1 with other archaeal and eukaryotic FEN1 homologs demonstrates that Tb-FEN1 displays 85%, 85%, 85%, 58%, 55%, 53%, 51%, 36%, 37% and 38% amino acid identity to the FEN1 homologs from *P. horikoshii*, *P. furiosus*, *T. kodakarensis*, *A. fulgidus*, *D. amylolyticus*, *S. solfataricus*, *M. jannaschii*, *Saccharomyces cerevisiae*, *Schizosaccharomyces pombe* and *Homo sapiens*, respectively. As shown in Fig. 1A, Tb-FEN1 possesses several highly conserved amino acids residues in the conserved motifs characteristic of the FEN1 homologs from other Archaea and eukaryotes, confirming that Tb-FEN1 resembles other FEN1 homologs, and should be capable of removing 5′-flap from DNA.

To biochemically characterize the enzyme, we cloned the Tb-FEN1 gene into the pET-28at-plus expression vector and further expressed its product in the *E. coli*

BL21(DE3) RIL cells. The recombinant Tb-FEN1 protein was successfully overexpressed with a 6 x His-tag at its C-terminus as a ~ 39 kDa protein (Fig. 1B). Using sonication, heat treatment (70°C for 20 min), and affinity chromatography with a Ni column, the recombinant Tb-FEN1 protein was purified to homogeneity (Fig. 1B).

3.2. Tb-FEN1 cleaves specifically 5′-flap DNA

We next employed the purified Tb-FEN1 to investigate whether this enzyme can cleave DNA by performing the DNA cleavage reactions using various DNA substrates. As shown in Fig. 2A, the 5′-flap DNA was gradually cleaved with increasing Tb-FEN1 protein concentrations at 45°C up to 91% cleavage percentage in the presence of 1000 nM Tb-FEN1, showing that the enzyme can effectively cleave 5′-flap DNA. In contrast, no cleaved product was observed using the pseudo Y DNA, no matter the Tb-FEN1 concentration used (Fig. 2B), which differs from other reported FEN1 homologs from Archaea and eukaryotes. Similarly, Tb-FEN1 had no activity towards normal ssDNA and dsDNA (Figs. 2C and 2D). Thus, these observations suggest that Tb-FEN1 can efficiently cleave 5′-flap DNA but not pseudo Y DNA.

3.3. Biochemical characteristics of Tb-FEN1

Since Tb-FEN1 can specifically cleave 5′-flap DNA, we employed the 5′-flap DNA as substrate to examine its thermostability, optimal pH, divalent metal ion requirement and salt tolerance. As shown in Fig. 3A, we demonstrated that the heated Tb-FEN1 protein retained 87%, 68%, and 71% cleavage activity after a 20 min treatment at 80°C, 85°C, and 90°C, respectively. Even after heating at 100°C for 20 min, Tb-FEN1 still possessed about 24% cleavage activity. Thus, Tb-FEN1 is a thermostable

endonuclease.

Moreover, we found that Tb-FEN1 can cleave 5′-flap DNA in a pH range from 6.5 to 9.5 with variable efficiencies (6.0-10.0) (Fig. 3B), demonstrating an optimal activity over a large pH range (7.0 to 9.0). In contrast, no activity was detected when the cleavage reactions of Tb-FEN1 were performed at pH 10 and pH 11. This observation is to take with caution since it might also result from the instability of the 5′-flap DNA under the high alkaline condition. Compared with Tb-FEN1, *T. kodakarensis* FEN1 has a relative narrow pH optimum range around 7.5 (Muzzamal et al., 2020), while that of *M. jannaschii* FEN was between 6 and 7, and pH 8 for the murine FEN-1 (Harrington and Liebern, 1994). Thus, the pH requirements of archaeal and eukaryotic FEN1 homologs may vary greatly depending on the source organism.

Next, we investigated whether the Tb-FEN1 activity is dependent on a divalent metal ion as observed for other FEM1 proteins. In the control reaction without a divalent metal ion, Tb-FEN1 had only residual activity (Fig. 3C, CK). This activity was further slightly reduced in the presence of 10 mM EDTA (Fig. 3C, EDTA), which confirms that the enzyme activity is dependent on a divalent metal ion. Tb-FEN1 exhibited its maximal activity in the presence of Mg^{2+}, and to almost the same extent in the presence of Mn^{2+}, which is similar to what is observed for the murine FEN1 (Zheng et al., 2002). Tb-FEN1 exhibited an extremely weak activity in the presence of Cu^{2+}, Zn^{2+} or Ca^{2+} and an intermediate activity in the presence of Co^{2+} and Ni^{2+}. In contrast to Tb-FEN1, Mn^{2+} greatly reduces the *M. jannaschii* FEN1 activity (Bae et al., 1999), and inhibits that of *T. kodakarensis* FEN1 (Muzzamal et al., 2020). Furthermore,

while the *T. kodakarensis* FEN1 activity is highest in the presence of Co^{2+} (Muzzamal et al., 2020), Tb-FEN1 retains only 25% relative activity with Co^{2+}, and while Cu^{2+} enables some activity with Tb-FEN1, it inhibits that of the *T. kodakarensis* FEN1 enzyme (Muzzamal et al., 2020). Reversely, Tb-FEN1 is inactive in the presence of Zn^{2+}, whereas it can activate the *T. kodakarensis* FEN1 activity (Muzzamal et al., 2020). Interestingly, no activity was observed for Tb-FEN1 and *T. kodakarensis* FEN1 in the presence of Ca^{2+} (Muzzamal et al., 2020). Thus, despite their high genetic proximity, the divalent metal ion requirements of Tb-FEN1 and *T. kodakarensis* FEN1 show more divergences than similarities.

Last, we investigated the effect of salinity on Tb-FEN1 activity. We show that the enzyme activity is inhibited by NaCl, abolishing its activity gradually with increasing NaCl concentrations (Fig. 3D). Specifically, Tb-FEN1 retained 40% cleavage activity at 200 mM NaCl, and only less than 20% cleavage at 400 mM or above. This is similar to what is observed for the *M. jannaschii* FEN1 (Bae et al., 1999), to the exception that Tb-FEN1 still retains ca. 13% relative activity at 600 mM NaCl, while *M. jannaschii* FEN1 has no detectable activity at and above 400 mM NaCl (Bae et al., 1999), suggesting that Tb-FEN1 is slightly more salt-tolerant than *M. jannaschii* FEN1. The difference in salt tolerance between these two FEN1 homologs cannot be related to the growth optima of the two strains, since both are marine hyperthermophilic isolates with optimal growth salinities ca. 3%, but it may be related to their central metabolism since *M. yannaschii* is a methanogen and *T. barophilus* is a peptidotrophe.

3.4. Thermostability mechanism assays

As shown in Fig. 1, we found that residues N30, I39, G153, A157, Q172, Y174, N187, L226, I227 and N238 in Tb-FEN1 are conserved in other FEN1 proteins from HA. In contrast, the corresponding residues in eukaryotic FEN1 proteins are the conserved methionine, valine, alanine, cysteine, glutamate, methionine, histidine, phenylalanine, valine, and cysteine (Fig. S1), respectively. To probe a link between these residues and the thermostability of Tb-FEN1, we mutated six residues in Tb-FEN1 back to the corresponding eukaryotic residue by site-directed mutagenesis: N30M, Q172E, Y174M, N187H, L226F and N238C, and purified these six mutant proteins (Fig. S2). We then tested their cleavage activity and thermostability. As shown in Fig. S3, we found that above five mutants displayed the wild-type 5'-flap DNA cleavage activity except for the N238C mutant. As shown in Fig. S4, the N30M, Q172E, Y174M, and N187H mutants exhibited wild-type thermostability. However, the L266F mutant displayed only 87% activity relative to the wild-type protein, suggesting that the L266 residue might play a role in the thermostability of Tb-FEN1.

3.5. Mutational analyses of Tb-FEN1

Tb-FEN1 possesses all conserved motifs present in FEN1 homologs from Archaea and eukaryotes, suggesting that this FEN1 resembles other archaeal and eukaryotic FEN1 proteins despite the biochemical specificities we demonstrated above. The human FEN1 is a well-characterized FEN1, and the solved crystal structure of the enzyme with the 5′-flap DNA demonstrates the amino acid residues of the human FEN1 that surround the flap (Fig. 4A) (Song et al., 2018). For clarity, the corresponding residues in Tb-FEN1 are shown in parentheses (Fig. 4A). To clarify the function of

these amino acid residues in Tb-FEN1, we have mutated five of the 9 conserved residues in the enzyme that are in the conserved motifs present in other FEN1 homologs. By using site-directed mutagenesis, we successfully engineered the Tb-FEN1 K87A, R94A, E154A, R186A and D236A mutants. These mutant proteins were expressed and purified as described for the wild-type protein (Fig. 4B).

The cleavage efficiencies of the Tb-FEN1 K87A, R94A, E154A, R186A and D236A mutants we determined by performing DNA cleavage reactions using 5′-flap DNA as a substrate. The Tb-FEN1 mutants K87A, R94A and E154A displayed no cleavage activity at all the tested protein concentrations (Figs. 5A, 5B and 5C), suggesting that the mutations of K87, R94 and E154 to alanine lead to the complete loss of activity. The Tb-FEN1 R186A mutant displayed wild-type cleavage efficiency (Fig. 5D), thereby indicating that this substitution to alanine has no detectable impact on enzyme activity. The Tb-FEN1 D236A mutant was the only mutant displaying reduced cleavage efficiencies (Fig. 5E) in comparison to the wild-type protein, emonstrating that the enzyme activity is only partially inhibited by the mutation of D236 to alanine. Thus, residue D236 is important for the enzyme to reach its full activity, but not essential for catalysis. Overall, our data suggest that residues K87, R94, and E154 in Tb-FEN1 are essential for cleaving 5′-flap DNA.

3.6. DNA-binding of the Wild-type/Mutant Tb-FEN1

To test whether the wild-type/mutant Tb-FEN1 proteins can bind 5′-flap DNA, we performed DNA binding assays by incubating the wild-type/mutant enzymes with the 5′-flap DNA substrate. As shown in Fig. 6A, the 5′-flap DNA substrate was gradually

bound with increasing wild-type protein concentrations. At 2.4 μM, binding reached 89%, thereby suggesting that Tb-FEN1 can bind effectively 5′-flap DNA.

In comparison, the K87A, R94A, E154A and D236A mutants displayed reduced binding efficiencies at all tested concentrations (Figs. 6B, 6C, 6D and 6F), demonstrating that residues K87, R94, E154 and D236 in Tb-FEN1 are involved in DNA substrate recognition and binding. The Tb-FEN1 R186A mutant had the lowest binding efficiency at 0.6 μM and 1.2 μM (Fig. 6E). However, the Tb-FEN1 R186A mutant displayed wild-type binding at 2.4 μM. Thus, it is probable that residue R186 is to involved directly in 5′-flap DNA substrate recognition but may participate in the proper folding of this site.

3.7. Kinetic analysis of Tb-FEN1

Under single-turnover condition where the enzyme concentration was ten-fold higher than DNA concentration, we performed a time course experiment of DNA cleavage catalyzed by Tb-FEN1 at 45ºC. As shown in Fig. 7A, the 5′-flap DNA substrate was gradually cleaved as the reaction time extended. Almost all the 5′-flap DNA substrate was cleaved by Tb-FEN1 when the reaction time reached 10 min or more, thereby indicating that the enzyme can cleave effectively 5′-flap DNA.

The molar amount of the remaining DNA substrate in the DNA cleavage reactions catalyzed by Tb-FEN1 was quantified and plotted against the reaction time and then fitting with a single-exponential decay equation to yield the k_{endo} and A values (Fig. 7B). The k_{endo} and A values were estimated to be 0.42 ± 0.04 min^{-1} and 89 ± 3 nM, respectively.

Similar kinetic experiments of 5′-flap DNA cleavage reactions catalyzed by Tb-FEN1 were performed at 25°C, 30°C, 35°C, and 40°C, respectively. The corresponding results are shown in Figs. S5, S6, S7, and S8 in supplementary data, respectively. The corresponding k_{endo} and A values are summarized in Table 2, demonstrating that the k_{endo} values increased as the reaction temperatures increased.

4. Discussion

Genomic analyses have shown that FEN1 is present in Eukarya and Archaea, and possesses an endonuclease/5′-3′ exonuclease activity that can remove 5′-flap from DNA. In the present work, we provide the biochemical characteristics and catalytic mechanism of the FEN1 from the hyperthermophilic euryarchaeon *T. barophilus* Ch5, demonstrating that Tb-FEN1 is indeed capable of effective excision of 5′-flap from DNA. However, the Tb-FEN1 exhibits several biochemical characteristics distinct from the reported FEN1 homologs from other HA.

4.1. Tb-FEN1 has no activity on pseudo Y DNA

In addition to removing 5′-flap from DNA, FEN1 can normally cleave efficiently pseudo Y DNA (Rao et al., 1998). However, to our surprise we found that Tb-FEN1 shows no activity towards the pseudo Y DNA at whatever concentration of the protein and substrate tested, which sharply contrasts with other FEN1 homologs from eukaryotes or other Archaea, even those from the genetically closely related species *P. horikoshii* and *P. furiosus* (Matsui et al., 1999; Hosfield et al., 1998a). Since Tb-FEN1 possesses 85% amino acid identity with *P. furiosus* FEN1, a question arose: why the former cannot cleave pseudo Y DNA but the latter can. The sequence comparison of

the amino acid sequences of Tb-FEN1 and other archaeal and eukaryotic FEN1 proteins shows that several differences might explain this divergence. Residue T126 in Tb-FEN1 is distinct from the conserved lysine or arginine in other archaeal and eukaryotic FEN1 proteins (Fig. 1A). Additionally, residue H159 in Tb-FEN1 is also different from the conserved tyrosine in archaeal FEN1 and alanine or glutamate in eukaryotic FEN1 (Fig. 1A). These residue differences might alter the ability of Tb-FEN1 to cleave pseudo Y DNA.

4.2. Tb-FEN1 has strong thermostability

Strong thermostability is a unique characteristic of proteins from hyperthermophiles. As expected since it originates from the hyperthermophilic euryarchaeon *T. barophilus* Ch5, Tb-FEN1 is quite thermostable. To our knowledge, it is the most thermostable among the reported FEN1 proteins, since it still retains activity after 20 min. at 100°C. Likewise, the FEN1 homolog from the hyperthermophilic archaeon *M. jannaschii* retained activity only up to 95°C for 15 min (Rao et al., 1998).

We probed the origin of the thermostability of Tb-FEN1, by substituting the amino acid composition of this endonuclease back to the non-thermostable human FEN1 (summarized in Tables S3). Recent studies have shown that thermophilic proteins have a higher percentage of hydrophobic amino acids than mesophilic ones (Panja et al., 2015). As shown in Table S3, the percentage (42.4%) of the hydrophobic amino acid (M, F, A, I, L, V, W and P) in Tb-FEN1 is higher than that in human FEN1 (39.6%). As claimed by Gamage et al. (2019), the proteins with the dipeptide composition-based Instability Index (II) value below 40 are stable proteins. Based on the ExPASy (Expert

Protein Analysis System), the II values of Tb-FEN1 and human FEN1 are computed to be 33.74 and 50.09, respectively, which further confirms that Tb-FEN1 should be more thermostable than the human FEN1. Additionally, the hyperthermophilic proteins possess an increased percentage of glutamate (E) and lysine (K) and a decreased percentage of glutamine (Q) and histidine (H), so that the E+K/Q+H ratio is >4.5 (Farias and Bonato, 2003). As expected, the E+K/Q+H ratio (5.34) in Tb-FEN1 is higher than that (2.7) in human FEN1.

In addition to amino acid composition, the conserved residues in FEN1 proteins from HA that are not conserved in eukaryotic FEN1 homologs might be a determinant for strong thermostability of hyperthermophilic archaeal FEN1 proteins. Such ten residues are present in hyperthermophilic archaeal FEN1 proteins (Fig.S1). Intriguingly, we revealed that only residue L266 in Tb-FEN1 seems to be partially responsible for the strong thermostability exhibited by the Tb-FEN1 protein. Considering that only a low reduction in activity (13%) was observed in the heated L266F mutant relative to the heated wild-type protein, we proposed that a network interaction of residue L266 and the other nine residues in hyperthermophilic archaeal FEN1 proteins might contribute to its thermostability.

4.3. Roles of the conserved residues in Tb-FEN1

Human FEN1 is a well-characterized structure-specific endonuclease. Residue D233 in human is essential for DNA substrate cleavage and binding (Shen et al., 1996). The corresponding residue D236 in *P. furiosus* FEN1 plays an important role in divalent metal ion binding (Allawi et al., 2003). In this work, our mutational studies showed that

the mutation of residue D236 in Tb-FEN1 to alanine leads to the partial loss of the catalytic activity and reduced binding efficiency, thereby confirming the role of the highly conserved aspartate residue in FEN1 homologs.

Residue E160 in human FEN1 is essential for DNA substrate cleavage and binding via Mg^{2+} coordination (Shen et al., 1997). In addition, the corresponding residue E154 in *P. furiosus* FEN1 may bridge the two metal ions through water-mediated contacts (Allawi et al., 2003). In this work, we confirmed that this highly conserved residue E154 in Tb-FEN1 is also essential for substrate cleavage and binding.

The mutation R192F in human FEN1 partially abolishes the cleavage activity (Song et al., 2018). In contrast, we found that the Tb-FEN1 R186A mutant retains wild-type activity. This difference might originate from the different amino acid substitutions used (Ala instead of Phe). Our binding data further demonstrate that residue R186 in Tb-FEN1 is possibly not directly involved in substrate recognition and binding.

The invariant basic residues K93 and R100 in human FEN1 form ion pairs with the scissile phosphate to facilitate hydrolysis (Tsutakawa et al., 2011). Similar observations are made for residue R94 in *P. furiosus* FEN1 (Allawi et al., 2003). In Tb-FEN1, residues K87 and R94 are analogous to residues K93 and R100 in human FEN1, respectively. In this work, we show that the K87A and R94A mutations lead to the loss of cleavage activity and a reduction in DNA substrate recognition and binding, which further confirms the function of the conserved basic amino acid residues.

4.4. Activation energy

In this work, the k_{endo} values for cleaving 5′-flap DNA by Tb-FEN1 were estimated

at various temperatures ranging from 25°C to 45°C. By using the Arrhenius equation, the log of k_{endo} values was plotted as a function of the reaction temperature to yield an activation energy (E_a) of 35.7 ± 4.3 kcal/mol (Fig. 8), which represents the energy barrier for the removal of 5′-flap from DNA. Under single-turnover conditions, other FEN homologs have been suggested to be rate-limited by conformational change rather than rate-limited by catalytic chemistry of phosphodiester bond hydrolysis (Kim et al., 1999; Kim et al., 2001; Zheng et al., 2002; Algasaier et al., 2016; Song et al., 2018). Therefore, the activation energy measured here could be an indication of the activation barrier for the conformational change rather than hydrolysis. To our knowledge, this is the first report on an activation energy (E_a) for 5′-flap removal from DNA by FEN1.

5. Conclusion

In summary, we investigated the biochemical characteristics of FEN1 from the hyperthermophilic euryarchaeon *T. barophilus* Ch5 and revealed the function of five conserved residues of the enzyme. Interestingly, Tb-FEN1 can remove 5′-flap from DNA, displaying maximal activity in the presence of Mg^{2+} at pH 7.0–9.5. However, Tb-FEN1 has no cleavage activity on pseudo Y DNA, which sharply contrasts with other eukaryotic and archaeal FEN1 homologs. Importantly, we found that Tb-FEN1 is the most thermostable among the reported FEN1 proteins. Additionally, we estimated for the first time the activation energy of DNA cleavage by Tb-FEN1 (35.7 ± 4.3 kcal/mol), which represents the energy barrier for the removal of 5′-flap from DNA. Mutational studies demonstrate that residues K87, R94, and E154 in Tb-FEN1 are essential for substrate binding and catalysis.

Author contributions

LZ and PO designed experiments; TL, DJ, LW, KC, LL, and ZL performed experiments; LZ, TL, WL, DJ, CJ and PO analyzed data; LZ and PO wrote and revised the paper.

Funding

This work was supported by the Provincial Natural Science Foundation of Jiangsu Province (No. BK20191219), High Level Talent Support Program of Yangzhou University and the Academic Leader of Middle and Young People of Yangzhou University Grant to LZ, and the Open Project of Jiangsu Key Laboratory of Marine Bioresources and Environments (No. SH20201206), Jiangsu Ocean University, China to CJ.

Declaration of Interest Statement

All authors declare that there is no conflict of interests regarding the publication of this paper.

Acknowledgements

We thank Prof. Yulong Shen at Shandong University for kindly providing the *E. coli* BL21 (DE3) RIL strains and Prof. Yong Gong at Institute of High Energy Physics, Chinese Academy of Sciences, China for kindly providing the pET-28at-plus vector.

Supplementary materials

Supplementary materials for this article are provided.

References

Algasaier, S.I., Exell, J.C., Bennet, I.A., Thompson, M.J., Gotham, V.J., Shaw, S.J., Craggs, T.D., Finger, L.D., Grasby, J.A., 2016. DNA and protein requirements for substrate conformational changes necessary for human flap endonuclease-1-catalyzed reaction. J. Biol. Chem. 291, 8258–8268.

Allawi, H.T., Kaiser, M.W., Onufriev, A.V., Ma, W.P., Brogaard, A.E., Case, D A., Neri, B.P., Lyamichev, V.I., 2003. Modeling of flap endonuclease interactions with DNA substrate. J. Mol. Biol. 328, 537–554.

Bae, K. W. Baek, K. W. Cho, C. S., Hwang, K. Y., Kim, H. R., Sung, H. C., Cho, Y., 1999. Expression, purification, characterization, and crystallization of flap endonuclease-1 from *Methanococcus jannaschii*. Mol. Cells 9, 45–48.

Balakrishnan, L., Bambara, R.A., 2013. Flap endonuclease. *Annu. Rev. Biochem.* 82, 119–138.

Bambara, R.A., Murante, R.S., Henricksen, L.A., 1997. Enzymes and reactions at the eukaryotic DNA replication fork. J. Biol. Chem. 272, 4647–4650.

Beattie, T.R., Bell, S.D., 2012. Coordination of multiple enzyme activities by a single PCNA in archaeal Okazaki fragment maturation. EMBO. J. 31, 1556–1567.

Burkhart, B.W., Cubonova, L., Heider, M.R., Kelman, Z., Reeve, J.N., Santangelo, T.J., 2017. The GAN exonuclease or the flap endonuclease Fen1 and RNase HII are necessary for viability of *Thermococcus kodakarensis*. J. Bacteriol. 199, e00141–17.

Ceska, T.A., Sayers, J.R., Stier, G., Suck, D., 1996. A helical arch allowing single-stranded DNA to thread through T5 5'- exonuclease. Nature 382, 90–93.

Chapados, B.R., Hosfield, D.J., Han, S. Qiu, J., Yelent, B., Shen, B., Tainer, J.A., 2004. Structural basis for FEN-1 substrate specificity and PCNA-mediated activation in DNA replication and repair. Cell 116, 39–50.

Collins, B.K., Tomanicek, S.J., Lyamicheva, N., Kaiser, M.W., Mueser, T.C., 2004. A preliminary solubility screen used to improve crystallization trials: crystallization and preliminary X-ray structure determination of *Aeropyrum pernix* flap endonuclease-1. Acta. Crystallogr. D. Biol. Crystallogr. 60, 1674–1678.

Dehé, P.M., Gaillard, P.H.L., 2017. Control of structure-specific endonucleases to maintain genome stability. Nat. Rev. Mol. Cell Biol. 18, 315−330.

Farias, S.T., Bonato, M.C., 2003. Preferred amino acids and thermostability. Genet Mol Res. 2, 383-393.

Finger, L.D., Atack, J.M., Tsutakawa, S., Classen, S., Tainer, J., Grasby, J., Shen, B., 2012. The wonders of flap endonucleases: structure, function, mechanism, and regulation. Subcell Biochem. 62, 301–326.

Gamage, D.G., Gunaratne, A., Periyannan, G.R., Russell, T.G., 2019. Applicability of instability index for in vitro protein stability prediction. Protein Pept. Lett. 26, 339-347.

Grasby, J.A., Finger, L.D., Tsutakawa, S.E., Atack, J.M., Tainer, J.A., 2012. Unpairing and gating: sequence-independent substrate recognition by FEN superfamily nucleases. Trends Biochem. Sci. 37, 74–84.

Guo, E., Ishii, Y., Mueller, J., Srivatsan, A., Gahman, T., Putnam, C. D., Wang, J.Y.J., Kolodner, R.D., 2020. FEN1 endonuclease as a therapeutic target for human cancers with defects in homologous recombination. Proc. Natl. Acad. Sci. USA 117, 19415–

19424.

Horie, M., Fukui, K., Xie, M., Kageyama, Y., Hamada, K., Sakihama, Y., Sugimori, K., Matsumoto, K., 2007. The N-terminal region is important for the nuclease activity and thermostability of the flap endonuclease-1 from *Sulfolobus tokodaii*. Biosci. Biotechnol. Biochem. 71, 855–865.

Hosfield, D.J., Frank, G., Weng, Y., Taineri, J.A. Shen, B., 1998a. Newly discovered archaebacterial flap endonucleases show a structure specific mechanism for DNA substrate binding and catalysis resembling human flap endonuclease-1. J. Biol. Chem. 273, 27154–27161.

Hosfield, D.J., Mol, C.D., Shen, B., Tainer, J.A., 1998b. Structure of the DNA repair and replication endonuclease and exonuclease FEN-1: coupling DNA and PCNA binding to FEN-1 activity. Cell 95, 135–146.

Hwang, K.Y., Baek, K., Kim, H.Y., Cho, Y., 1998. The crystal structure of flap endonuclease-1 from *Methanococcus jannaschii*. Nature Struct. Biol. 5, 707–713.

Kikuchi, K., Taniguchi, Y., Hatanaka, A., Sonoda, E., Hochegger, H., Adachi, N., Matsuzaki, Y., Koyama, H., Van Gent, D. C., Jasin, M., Takeda, S., 2005. FEN-1 facilitates homologous recombination by removing divergent sequences at DNA break ends. Mol. Cell Biol. 25, 6948–6955.

Kim, C.Y., Park, M.S., Dyer, R.B., 2001. Human flap endonuclease-1: conformational change upon binding to the flap DNA substrate and location of the Mg^{2+} binding site. Biochemistry 40, 3208–3214.

Kim, C.Y., Shen, B., Park, M.S., Olah, G.A., 1999. Structural changes measured by X-ray scattering from human flap endonuclease-1 complexed with Mg^{2+} and flap DNA substrate. J Biol Chem. 274, 1233–1239.

Klungland, A., Lindahl, T., 1997. Second pathway for completion of human DNA base excision-repair: reconstitution with purified proteins and requirement for DNase IV (FEN1). EMBO J. 16, 3341–3348.

Lieber, M.R., 1997. The FEN-1 family of structure-specific nucleases in eukaryotic DNA replication, recombination, and repair. Bioessays 19, 233–240.

Liu, S., Lu, G., Ali, S., Liu, W., Zheng, L., Dai, H., Li, H., Xu, H., Hua, Y., Zhou, Y., Ortega, J., Li, G. M., Kunkel, T. A., Shen, B., 2015. Okazaki fragment maturation involves alpha-segment error editing by the mammalian FEN1/MutSalpha functional complex. EMBO J. 34, 1829−1843.

Marteinsson, V.T., Birrien, J.L., Reysenbach, A., Vernet, L.M., Marie, D., Gambacorta, A., Messner, P., Sleytr, U.B., Prieur, D., 1999. *Thermococcus barophilus* sp. nov., a new barophilic and hyperthermophilic archaeon isolated under high hydrostatic pressure from a deep-sea hydrothermal vent. Int. J. Syst. Bacteriol. 49, 351–359.

Mase, T., Kubota, K., Miyazono, K., Kawarabayasi, Y., Tanokura, M., 2011. Structure of flap endonuclease 1 from the hyperthermophilic archaeon *Desulfurococcus amylolyticus*. Acta. Crystallogr. Sect. F. Struct. Biol. Cryst. Commun. 67, 209–213.

Matsui, E., Kawasaki, S., Ishida, H., Ishikawa, K., Kosugi, Y., Kikuchi, H., Kawarabayashi, Y., Matsui, I., 1999. Thermostable flap endonuclease from the archaeon, *Pyrococcus horikoshii*, cleaves the replication fork-like structure

endo/exonucleolytically. J. Biol. Chem. 274, 18297–18309.

Matsui, E., Musti, K. V., Abe, J., Yamasaki, K., Matsui, I., Harata, K., 2002. Molecular structure and novel DNA binding sites located in loops of flap endonuclease-1 from *Pyrococcus horikoshii*. J. Biol. Chem. 277, 37840–37847.

Matsui, E., Urushibata, Y., Abe, J., Matsui, I., 2014. Serial intermediates with a 1 nt 3'-flap and 5' variable-length flaps are formed by cooperative functioning of *Pyrococcus horikoshii* FEN-1 with either B or D DNA polymerases. Extremophiles 18, 415–427.

Murante, R.S., Rust, L., Bambara, R.A., 1995. Calf 5' to 3' exo/endonuclease must slide from a 5' end of the substrate to perform structure-specific cleavage. J. Biol. Chem. 270, 30377–30383.

Muzzamal, H., Ain, Q.U., Saeed, M.S., Rashid, N., 2020. Gene cloning and characterization of Tk1281, a flap endonuclease 1 from *Thermococcus kodakarensis*. Folia Microbiol (Praha) 62, 407–415.

Oger, P., Sokolova, T.G., Kozhevnikova, D.A., Taranov, E. A., Vannier, P., Lee, H.S., Kwon, K.K., Kang, S.G., Lee, J.H., Bonch-Osmolovskaya, E.A.A., Lebedinsky, V., 2016. Complete genome sequence of the hyperthermophilic and piezophilic archaeon *Thermococcus barophilus* Ch5, capable of growth at the expense of hydrogenogenesis from carbon monoxide and formate. Genome Announc. 4, e01534-15.

Panja, A.S., Bandopadhyay, B., Maiti, S., 2015. Protein thermostability is owing to their preferences to non-polar smaller volume amino acids, variations in residual physico-chemical properties and more salt-bridges. PLoS One 10, e0131495.

Rao, H.G., Rosenfeld, A., Wetmur, J.G., 1998. *Methanococcus jannaschii* flap

endonuclease: expression, purification, and substrate requirements. J Bacteriol. 180, 5406-5412.

Shen, B., Qiu, J., Hosfield, D., Tainer, J.A., 1998. Flap endonuclease homologs in archaebacteria exist as independent proteins. Trends Biochem. Sci. 23, 171–173.

Shen, B., Nolan, J.P., Sklar, L.A., Park, M.S., 1996. Essential amino acids for substrate binding and catalysis of human flap endonuclease 1. J. Biol. Chem. 271, 9173–9176.

Shen, B., Nolan, J.P., Sklar, L.A., Park, M.S., 1997. Functional analysis of point mutations in human flap endonuclease-1 active site. Nucleic Acids Res. 25, 3332–3338.

Shi, Y., Hellinga, H.W., Beese, L.S., 2017. Interplay of catalysis, fidelity, threading, and processivity in the exo- and endonucleolytic reactions of human exonuclease I. Proc. Natl. Acad. Sci. USA 114, 6010–6015.

Song, B., Hamdan, S.M., Hingorani, M.M., 2018. Positioning the 5'-flap junction in the active site controls the rate of flap endonuclease-1-catalyzed DNA cleavage. J. Biol. Chem. 293, 4792–4804.

Storici, F., Henneke, G., Ferrari, E., Gordenin, D.A., HuÈbscher, U., Resnick, M.A., 2002. The flexible loop of human FEN1 endonuclease is required for flap cleavage during DNA replication and repair. EMBO J. 21, 5930–5942.

Tsutakawa, S.E., Classen, S., Chapados, B.R., Arvai, A.S., Finger, L.D., Guenther, G., Tomlinson, C., Thompson, G.P., Sarker, A.H., Shen, B., Cooper, P.K., Grasby, J.A., Tainer, J.A., 2011. Human flap endonuclease structures, DNA double-base flipping, and a unified understanding of the FEN1 superfamily. Cell 145, 198–211.

Tsutakawa, S.E., Thompson, M.J., Arvai, A.S., Neil, A.J., Shaw, S.J., Algasaier, S.I.,

Kim, J.C., Finger, L.D., Jardine, E., Gotham, V.J.B., Sarker, A.H., Her, M.Z., Rashid, F., Hamdan, S.M., Mirkin, S.M., Grasby, J.A., Tainer, J.A., 2017. Phosphate steering by flap endonuclease 1 promotes 5'-flap specificity and incision to prevent genome instability. Nat. Commun. 8, 15855.

Varshney, G.K., Burgess, S.M., 2016. DNA-guided genome editing using structure-guided endonucleases. Genome Biol. 17, 187.

Wu, X., Wilson, T.E., Lieber, M.R., 1999. A role for FEN-1 in nonhomologous DNA end joining: the order of strand annealing and nucleolytic processing events. Proc. Natl. Acad. Sci. USA 96, 1303−1308.

Xu, S., Cao, S., Zou, B., Yue, Y., Gu, C., Chen, X., Wang, P., Dong, X., Xiang, Z., Li, K., Zhu, M., Zhao, Q., Zhou, G., 2016. An alternative novel tool for DNA editing without target sequence limitation: the structure-guided nuclease. Genome Biol. 17, 186.

Zhao, E., Zhou, C., Chen, S., 2020. Flap endonuclease 1 (FEN1) as a novel diagnostic and prognostic biomarker for gastric cancer. Clin. Res. Hepatol. Gastroenterol. 45, 101455.

Zheng, L., Jia, J., Finger, L. D., Guo, Z., Zer, C., Shen, B., 2011. Functional regulation of FEN1 nuclease and its link to cancer. Nucleic Acids Res. 39, 781−794.

Zheng, L., Li, M., Shan, J., Krishnamoorthi, R., Shen, B., 2002. Distinct roles of two Mg^{2+} binding sites in regulation of murine flap endonuclease-1 activities. Biochemistry 41, 10323–10331.

Figure legends

Fig. 1. **The genome of *T. barophilus* Ch5 encodes a putative FEN1.** A. Sequence alignment of FEN1s from archaea and eukaryotes. Tba: *Thermococcus barophilus* (NCBI reference sequence: WP_056933915); Pho: *Pyrococcus horikoshii* (UniProtKB reference sequence: O50123); Pfu: *Pyrococcus furiosus* (UniProtKB reference sequence: O93634); Tko: *Thermococcus kodakarensis* (UniProtKB reference sequence: Q5JGN0); Afu: *Archaeoglobus fulgidus* (UniProtKB reference sequence: O29975); Dam: *Desulfurococcus amylolyticus* (Genbank reference sequence: AFL67054.1); Sso: *Sulfolobus solfataricus* (UniProtKB reference sequence: Q980U8); Mja: *Methanocaldococcus jannaschii* (UniProtKB reference sequence: Q58839); Sce: *Saccharomyces cerevisiae* (Genbank reference sequence: GFP67859); Spo: *Schizosaccharomyces pombe* (UniProtKB/Swiss-Prot: P39750); Hsa: *Homo sapiens* (NCBI reference sequence: P39748). The secondary-structure assignment of *P. furiosus* FEN1 (PDB entry 1b43), the closest Tb-FEN1 homolog, is shown by helices (α-helices) and arrows (β-strands). Highly conserved residues in the active site of human FEN1 are indicated by solid triangle. Flexible loop is shown by magenta box. The conserved amino acid residues are colored blue. Similar amino acid residues are boxed. The mutated residues are labeled with "*". B. Overexpression and purification of Tb-FEN1. The Tb-FEN1 protein was induced for expression by the addition of IPTG and purified following sonication, heat treatment (70^{o}C for 20 min) and Ni column affinity purification.

Fig. 2. DNA cleavage by Tb-FEN1. DNA cleavage reactions were performed with 300, 600 and 1000 nM Tb-FEN1 at 45°C for 30 min using various DNA substrates, respectively. A. Cleavage of 5′-flap DNA. B. Cleavage of pseudo Y DNA. C. Cleavage of ssDNA. D. Cleavage of dsDNA. CK: the DNA cleavage reaction without enzyme.

Fig. 3. Biochemical characteristics of Tb-FEN1. The 5′-flap DNA cleavage reactions of Tb-FEN1 were performed under various conditions. A. Thermostability assays. B. Effect of pH on the enzyme activity. C. Effect of divalent metal ion on the enzyme activity. D. Effect of NaCl concentrations on the enzyme activity.

Fig. 4. Potentially key amino acid residues of Tb-FEN1 that surround the 5′-flap. A. The human FEN1-substrate complex (5UM9) shows DNA distortion at the flap junction (Song et al., 2018). This figure was adapted from Song et al. (2018). The 5′-flap DNA is colored with orange and the residues are labeled with sticks. Residues D34 and D86 coordinate metal ion B and Residues D181 and D233 coordinate metal ion A. The corresponding amino acids of Tb-FEN1 are shown in the parentheses. B. Purification of the Tb-FEN1 K87A, R94A, E154A, R186A, and D236A mutants.

Fig. 5. Cleavage of 5′-flap DNA catalyzed by the Tb-FEN1 mutants. The 5′-flap DNA cleavage reactions of the Tb-FEN1 mutants were performed in the presence of 300 nM, 600 nM, and 1000 nM at 45°C for 30 min, respectively. Reaction products were separated by electrophoresis. A. The K87A mutant. B. The R94A mutant. C. The E154A mutant. D. The R186A mutant. E. The D236A mutant. CK: the reaction without enzyme.

Fig. 6. DNA-binding by the wild-type/mutant Tb-FEN1. The 5′-flap DNA was incubated with the wild-type and mutants of Tb-FEN1 with varied concentrations at 25°C for 10 min. The bound product was separated from free DNA by electrophoresis. A. DNA binding by the wild-type protein. B. DNA binding by the K87A mutant. C. DNA binding by the R94A mutant. D. DNA binding by the E154A mutant. E. DNA binding by the R186A mutant. F. DNA binding by the D236A mutant. CK: the DNA binding assay without enzyme.

Fig. 7. Kinetic analysis of DNA cleavage catalyzed by Tb-FEN1 at 45°C. DNA cleavage reactions of Tb-FEN1 were performed using 100 nM 5′-flap DNA as substrate in the presence of 1000 nM enzyme at 45°C for various times (10 s - 30 min) at 45°C. A. DNA cleavage reactions of Tb-FEN1. B. Determination of the reaction rate of DNA cleavage by Tb-FEN1. The amount of remaining substrate was plotted as a function of time by the single exponential decay equation to yield a reaction rate (k_{endo}) of 0.42 ± 0.04 (min^{-1}). CK: the reaction without enzyme.

Fig. 8. Activation energy for DNA cleavage catalyzed by Tb-FEN1. Ln (k_{endo}) was plotted as a function of the treated reciprocal of reaction temperature (1000/K) by a linear regression originated from the Arrhenius equation to yield an activation energy (E_a) of 35.7 ± 4.3 kcal/mol.

Table 1 Sequences of the oligonucleotides used to clone the Tb-FEN1 gene and construct its mutants

Name	Sequence (5′-3′)
Tb-FEN1 F	CGC*GGATCC*ATGGGAGTTCAGATAGGTGAG
Tb-FEN1 R	CCG*CTCGAG*TCATTTCTTTCTCATGAACCA
N30M F	AGCCATTGATGCTTTAATGGCAATTTATCAGT
N30MR	CATTAAAGCATCAATGGCTATCTTCCTTCCGT
K87A F	GAAAGCCGCCAGAATTCGCGAAGAAGGAGCTT
K87A R	GCGAATTCTGGCGGCTTTCCATCAAAGACATA
R94A F	AGAAGGAGCTTGAAAAAGCAGCGGAAGCAAGG
R94A R	GCTTTTTCAAGCTCCTTCTTCTTGAATTCTGG
E154A F	GGCTCCGAGTGAAGGTGCGGCTCAAGCGGCT
E154A R	GCACCTTCACTCGGAGCCTGCACCCATGGAA
Q172E F	TCTGGGCTTCAGCTTCTGAGGATTATGACTC
Q172E R	CAGAAGCTGAAGCCCAGACTTTACCCTTTGA
Y174M F	CTTCAGCTTCTCAGGATATGGACTCACTTTTGT
Y174MR	CATATCCTGAGAAGCTGAAGCCCAGACTTTACC
R186A F	GAGCACCAAGGCTTGTTGCGAATTTGACAATA
R186A R	GCAACAAGCCTTGGTGCTCCAAACAAAAGTGA
N187H F	CACCAAGGCTTGTTAGGCATTTGACAATAAC
N187H R	GCCTAACAAGCCTTGGTGCTCCAAACAAAAG
L226F F	AAATTGACAGGGAAAAGTTCATAGAACTTGC
L226F R	ACTTTTCCCTGTCAATTTTCAGTTCTTTTAG
D236A F	TATTCTGGTTGGAACGGCTTATAATCCAGGT
D236A R	GCCGTTCCAACCAGAATAGCAAGTTCTATGA
N238C F	TGGTTGGAACGGATTATTGTCCAGGTGGCATT
N238C R	CAATAATCCGTTCCAACCAGAATAGCAAGTTC

The italic bases represent restriction sites.

The substitution bases are underlined.

Table 2 Kinetic constants for cleaving 5′-flap DNA by Tb-FEN1 at varied temperatures

Temperature (°C)	k_{endo} (min^{-1})	A (nM)
25	0.0079 ± 0.005	80 ± 1
30	0.029 ± 0.002	93 ± 3
35	0.072 ± 0.01	86 ± 5
40	0.13 ± 0.02	80 ± 3
45	0.42 ± 0.04	89 ± 3

Figure 1

A

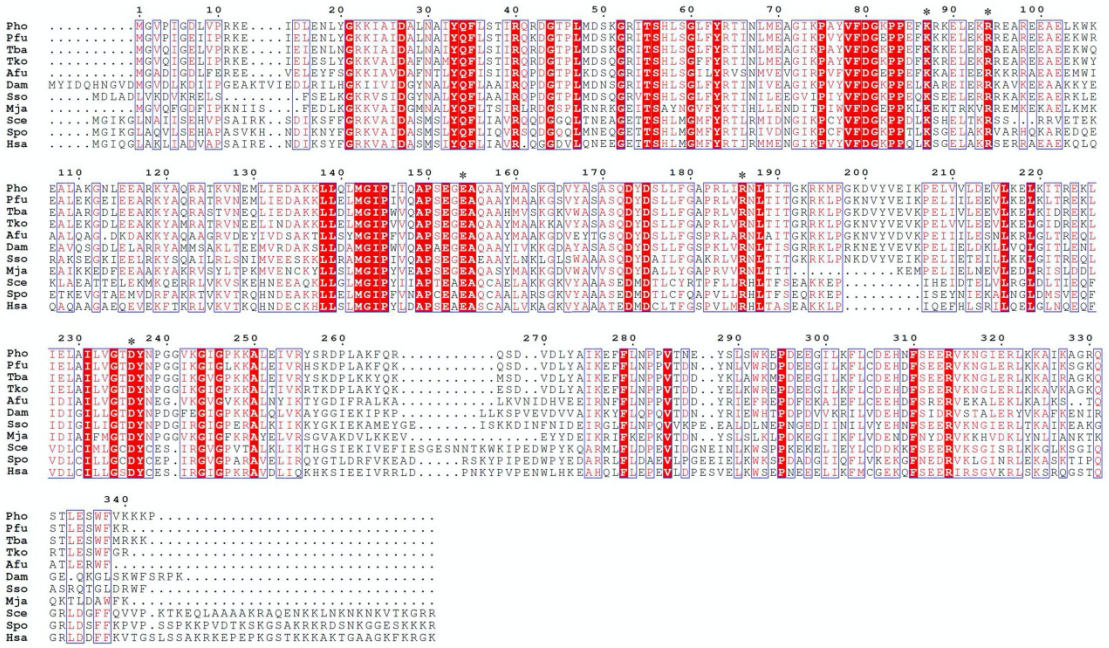
Pho
Pfu
Tba
Tko
Afu
Dam
Sso
Mja
Sce
Spo
Hsa

B

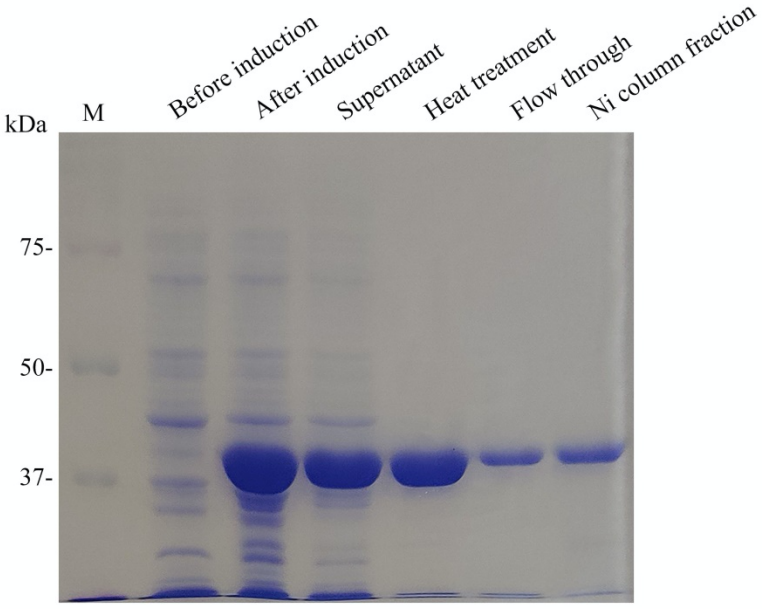
kDa
M
Before induction
After induction
Supernatant
Heat treatment
Flow through
Ni column fraction
75-
50-
37-

Figure 2

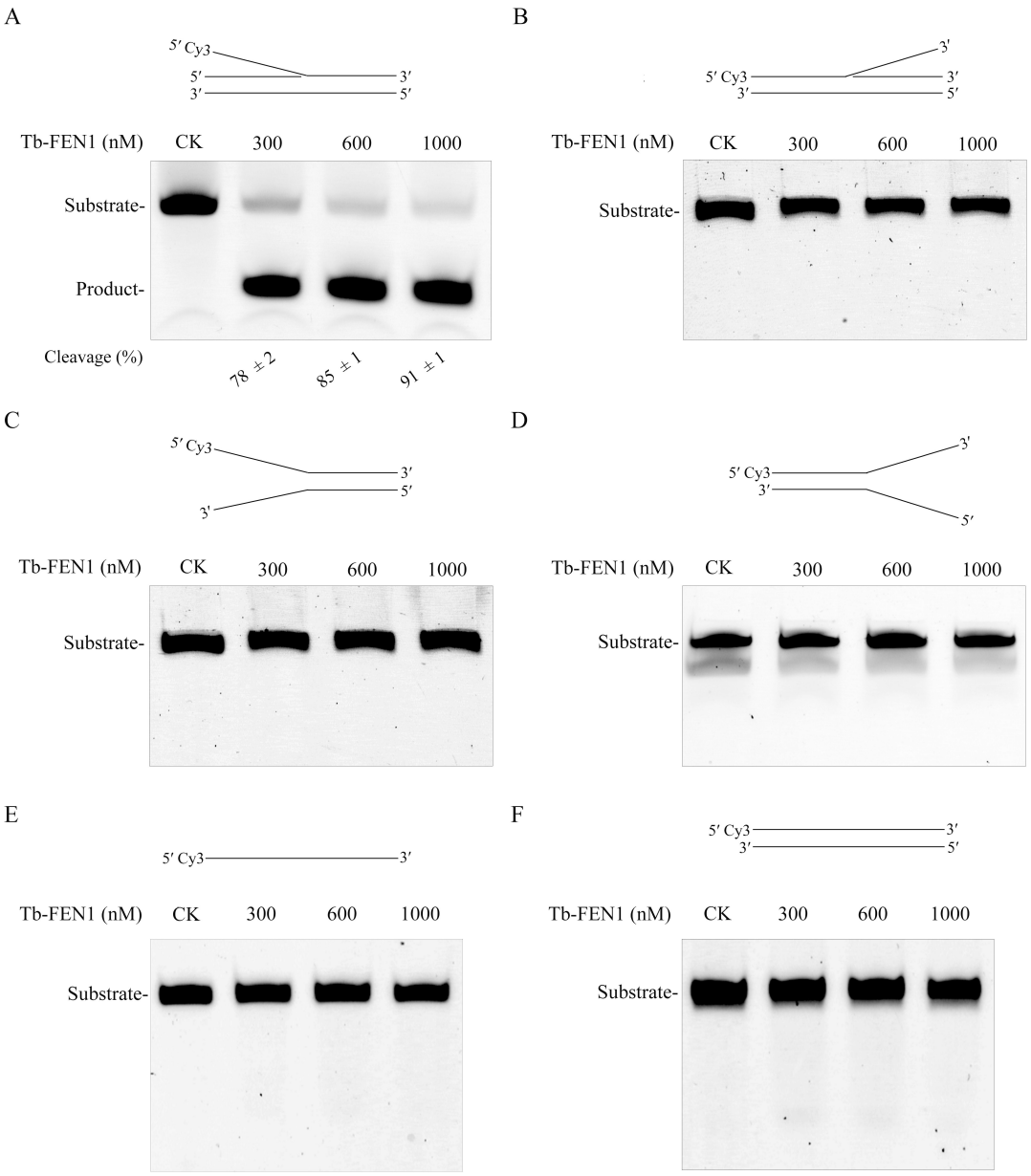
A
5′ Cy3
5′
3′
3′
5′
Tb-FEN1 (nM)
CK
300
600
1000
Substrate-
Product-
Cleavage (%)
78 ± 2
85 ± 1
91 ± 1
B
3′
5′ Cy3
3′
5′
Tb-FEN1 (nM)
CK
300
600
1000
Substrate-
C
5′ Cy3
3′
5′
3′
Tb-FEN1 (nM)
CK
300
600
1000
Substrate-
D
3′
5′ Cy3
3′
5′
Tb-FEN1 (nM)
CK
300
600
1000
Substrate-
E
5′ Cy3
3′
Tb-FEN1 (nM)
CK
300
600
1000
Substrate-
F
5′ Cy3
3′
3′
5′
Tb-FEN1 (nM)
CK
300
600
1000
Substrate-

Figure 3

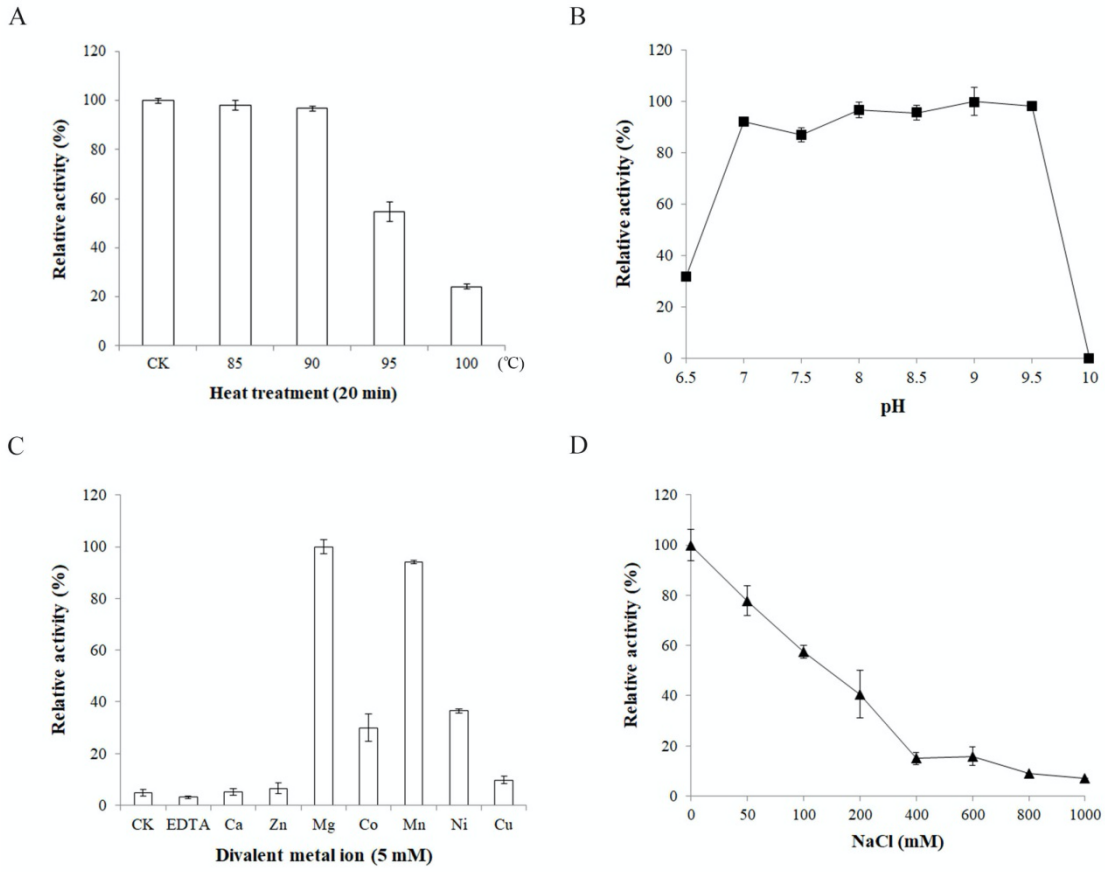
A
Relative activity (%)
120
100
80
60
40
20
0
CK
85
90
95
100
(℃)
Heat treatment (20 min)
B
Relative activity (%)
120
100
80
60
40
20
0
6.5
7
7.5
8
8.5
9
9.5
10
pH
C
Relative activity (%)
120
100
80
60
40
20
0
CK
EDTA
Ca
Zn
Mg
Co
Mn
Ni
Cu
Divalent metal ion (5 mM)
D
Relative activity (%)
120
100
80
60
40
20
0
0
50
100
200
400
600
800
1000
NaCl (mM)

Figure 4

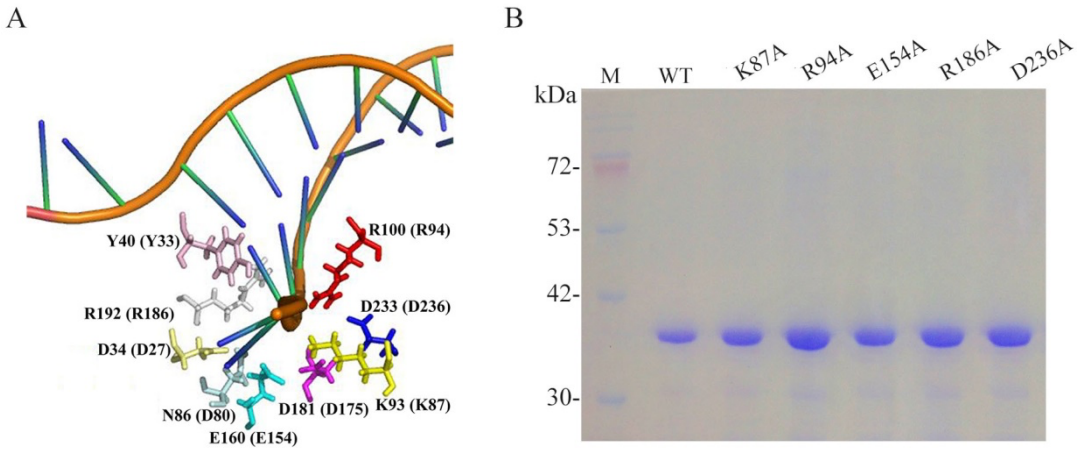
A
Y40 (Y33)
R100 (R94)
R192 (R186)
D233 (D236)
D34 (D27)
N86 (D80)
D181 (D175)
K93 (K87)
E160 (E154)
B
M
WT
K87A
R94A
E154A
R186A
D236A
kDa
72-
53-
42-
30-

Figure 5

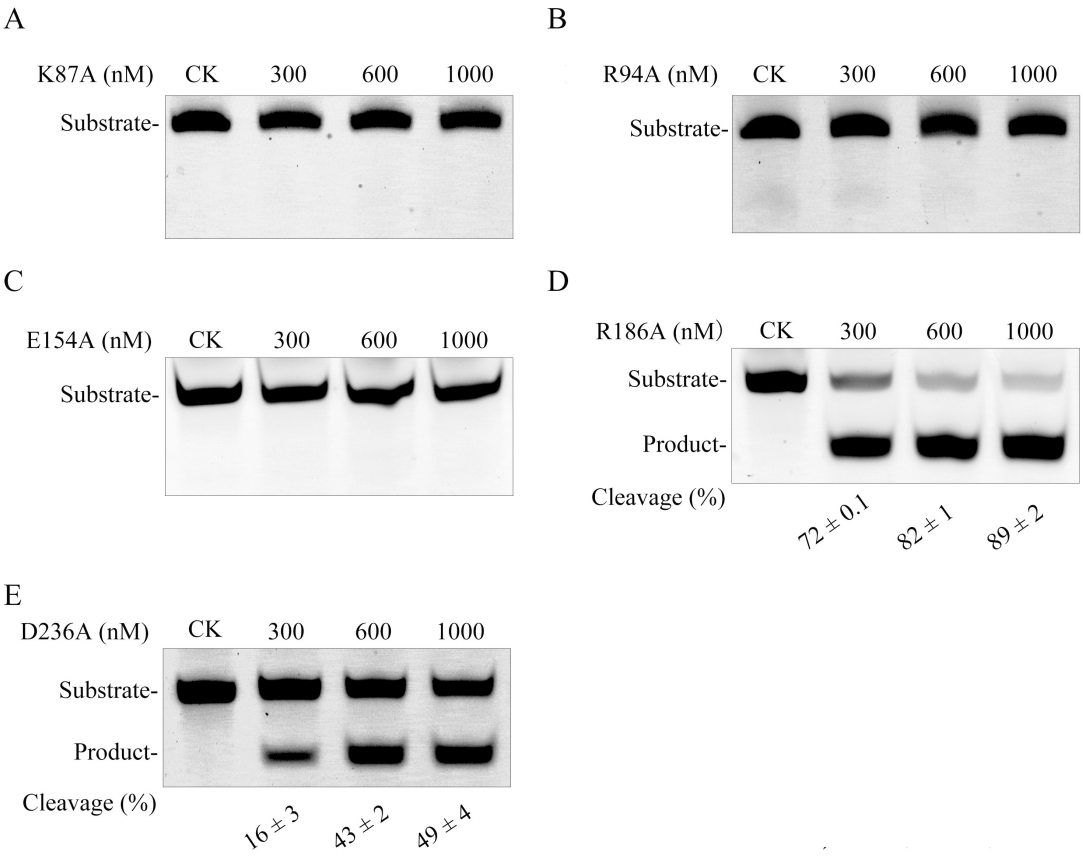
A
K87A (nM) CK 300 600 1000
Substrate-
B
R94A (nM) CK 300 600 1000
Substrate-
C
E154A (nM) CK 300 600 1000
Substrate-
D
R186A (nM) CK 300 600 1000
Substrate-
Product-
Cleavage (%)
72 ± 0.1
82 ± 1
89 ± 2
E
D236A (nM) CK 300 600 1000
Substrate-
Product-
Cleavage (%)
16 ± 3
43 ± 2
49 ± 4

Figure 6

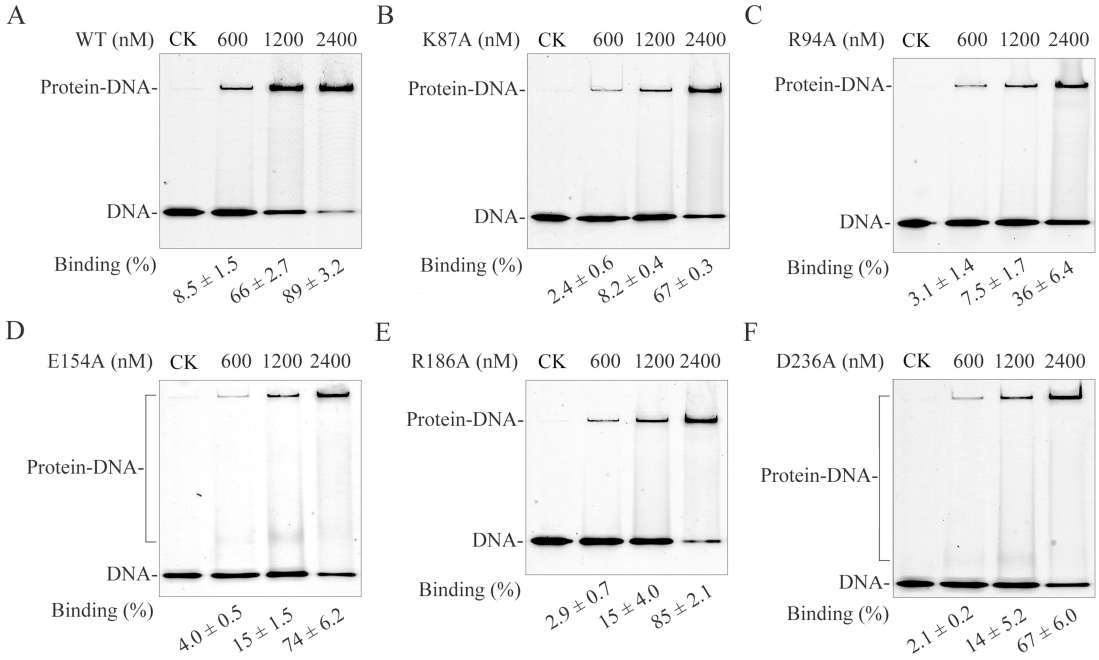
A
WT (nM) CK 600 1200 2400
Protein-DNA-
DNA-
Binding (%)
8.5 ± 1.5
66 ± 2.7
89 ± 3.2
B
K87A (nM) CK 600 1200 2400
Protein-DNA-
DNA-
Binding (%)
2.4 ± 0.6
8.2 ± 0.4
67 ± 0.3
C
R94A (nM) CK 600 1200 2400
Protein-DNA-
DNA-
Binding (%)
3.1 ± 1.4
7.5 ± 1.7
36 ± 6.4
D
E154A (nM) CK 600 1200 2400
Protein-DNA-
DNA-
Binding (%)
4.0 ± 0.5
15 ± 1.5
74 ± 6.2
E
R186A (nM) CK 600 1200 2400
Protein-DNA-
DNA-
Binding (%)
2.9 ± 0.7
15 ± 4.0
85 ± 2.1
F
D236A (nM) CK 600 1200 2400
Protein-DNA-
DNA-
Binding (%)
2.1 ± 0.2
14 ± 5.2
67 ± 6.0

Figure 7

A

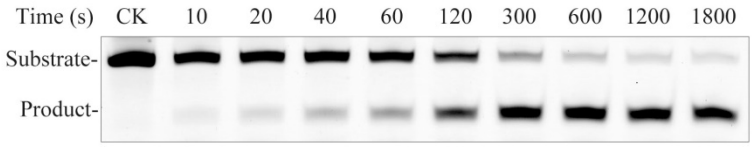
Time (s) CK 10 20 40 60 120 300 600 1200 1800
Substrate-
Product-

B

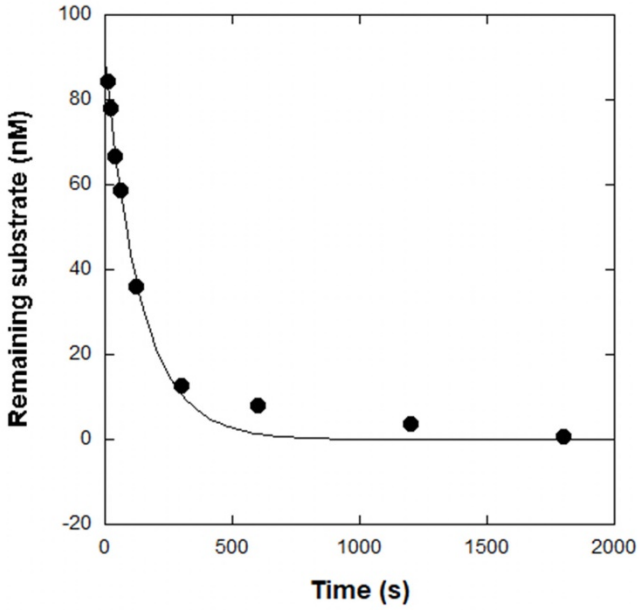
Remaining substrate (nM)
Time (s)
100
80
60
40
20
0
-20
0
500
1000
1500
2000

Figure 8